PROCEEDINGS OF THE 33rd European Symposium on Computer Aided Process Engineering (ESCAPE33), June 18-21, 2023, Athens, Greece

Effect of coalescence models on the prediction of the separation of dispersed oil-water pipe flows

Nikola Evripidou[a], Federico Galvanin[b], Panagiota Angeli[a]

[a] *ThAMeS Multiphase, Department of Chemical Engineering, University College London, London WC1E 7JE, UK*

[b] *Department of Chemical Engineering, University College London, London WC1E 7JE, UK*

Abstract

The effect of coalescence models on the prediction of the separation of dispersed oil-water pipe flows was assessed using a one-dimensional mechanistic model. The mechanistic model predicts the formation and evolution of four characteristic layers along the pipe: a pure water layer at the bottom, a flotation/sedimentation layer, a dense-packed zone, and a pure oil layer on the top. It was shown that the film drainage coalescence model by Jeelani and Hartland (1994) that considers interfacial mobility produces good predictions at low mixture velocity, but it depends on the flowrate. The asymmetric film drainage coalescence model by Henschke et al. (2002) is independent of the mixture velocity and the dispersed-phase fraction, and produces reasonable predictions. There was small deviation between the model outputs in the presence of the four characteristic layers, but further investigation of the regions where a single dense-packed layer persists is required.

Keywords: coalescence; liquid-liquid; dispersion; separation; modelling

1. Introduction

Liquid-liquid pipe flows are common in the petroleum industry. Deepwater and marginal fields with lower volumes of reserve entail new development challenges, while heavy oils and mature wells require water flooding to enhance production. Increased volumes of water in the pipelines affect the flow, as they can alter the spatial configuration of the two immiscible phases. Considering the high cost associated with oil extraction and separation, as well as the increased demands for further offshore drilling, ensuring a successful and economical flow of oil-water mixtures is essential in optimising transportation and downstream separation of the extracted oil. Additionally, subsea separation facilities are used to reduce the cost and space requirements of remote deepwater operations. The oil-water flows in pipes are often in the dispersed pattern. Models that can predict flow pattern transitions in unstable dispersed pipe flows are essential during both design and operation of industrial facilities.

Henschke et al. (2002) developed a mechanistic model that predicts the evolution of heights of the characteristic layers that develop in separating batch dispersions as well as the average drop size. The model uses coalescence time correlations based on asymmetrical film drainage between the drops. Pereyra et al. (2013) attempted to extend Henschke's model to one-dimensional pipe flows by changing the time scale to a length scale. Evripidou et al. (2019) further modified the model to account for hindered settling of drops in dense dispersions. Another coalescence model was proposed by Jeelani and Hartland (1994) and is based on the interfacial mobility. In this work, we use the mechanistic model as presented in Evripidou et al. (2019). We consider both the *asymmetric film drainage coalescence model* by Henschke et al. (2002) and the *interfacial mobility film drainage coalescence model* by Jeelani and Hartland (1994), to assess their ability to predict the formation and evolution of the characteristic layers in a pipe, for different oil-in-water dispersed flows.

2. Model description

Four characteristic layers may emerge in a separating dispersed pipe flow. In an oil-in-water dispersion, these are a pure water layer at the bottom, a settling layer (SL), a dense-packed layer (DPL), and a pure oil layer at the top. Figure 1 shows schematically these layers. The thickness of each layer depends on the drop settling (flotation/sedimentation) rate and the coalescence rate of drops, with their homophase. The drop size may also change through drop-drop coalescence.

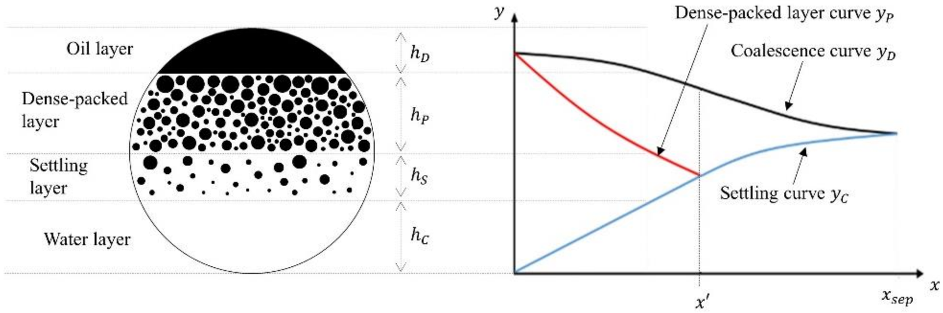

Figure 1: Diagram of the cross-sectional area of the pipe for an oil-in-water dispersion and diagram of the evolution of the characteristic layers.

The mechanistic model is applicable to liquid-liquid pipe flows where the separation is primarily gravity-driven. A constant mixture velocity, u_{M}, is assumed for both phases – this allows velocity profiles to be ignored, which means that there is no exchange of momentum between layers. For the dispersed layers, monodisperse drop distributions are assumed for simplification, while interfacial tension is considered constant. Lastly, drop break-up and turbulence effects are neglected. In what follows, the model equations associated with coalescence are briefly discussed.

2.1. Coalescence analysis

2.1.1. Drop-interface coalescence

Accumulation of drops near the top of the pipe results in coalescence and the formation of a pure oil layer of thickness h_D. Assuming a monodispersed DPL with drops of diameter $d_{p,I}$,

$$\frac{dh_D}{dx} = \frac{2\varphi_I d_{p,I}}{3\tau_I u_M}, \tag{1}$$

where τ_{I} is the drop-interface coalescence time. The oil fraction at the interface φ_I is approximately 1.

2.1.2. Drop-drop coalescence

Drop-drop coalescence is considered only in the DPL. Assuming that in each step, all drops within the DPL are of equal size, $d_{p,I}$,

$$\frac{\mathrm{d}(\mathrm{d_{p,I}})}{\mathrm{dx}} = \frac{\mathrm{d_{P,I}}}{6\tau_{\mathrm{C}}\mathrm{u_M}}. \tag{2}$$

where τ_C is the drop-drop coalescence time.

2.1.3. Coalescence time

Two coalescence models are considered. These are outlined in table 1. $d_{p,0}$ is the drop size at the inlet, μ is viscosity, ρ is t density, σ is the interfacial tension whereas the subscripts C and D refer to the continuous and dispersed phases respectively; g is the gravitational constant.

Table 1: Coalescence models

Asymmetric film drainage model	*Interfacial mobility film drainage model*
Drop-interface coalescence time: $\tau_I = \frac{(6\pi)^{\frac{7}{6}}\mu_C\, r_a^{\frac{7}{3}}}{4\sigma^{\frac{5}{6}}\, \mathrm{H}^{\frac{1}{6}}\, r_{F,I} r_V^*}$ (3)	Drop-interface coalescence time: $\tau_I = \frac{\tau_{I,0} d_{p,I}}{h_P}$ (9)
Drop-drop coalescence time: $\tau_C = \frac{(6\pi)^{\frac{7}{6}}\mu_C\, r_a^{\frac{7}{3}}}{4\sigma^{\frac{5}{6}}\, \mathrm{H}^{\frac{1}{6}}\, r_{F,C} r_V^*}$ (4)	Drop-drop coalescence time: $\tau_{I,0} = \frac{3\pi\mu_C r^4}{4(1+2m)F\delta_r^2}$ (10)
Drop-drop contact radius: $r_{F,C} = 0.3025 d_{p,I}\sqrt{1-\frac{4.7}{La+4.7}}$ (5)	Modified coalescence equation: $\frac{dh_D}{dx} = \frac{2\varphi_I h_P}{3\tau_{I,0} u_M}$ (11)
Drop-interface contact radius: $r_{F,I} = \sqrt{3} r_{F,C}$ (6)	Drop-interface film radius: $r = d_{p,0}^2\sqrt{\frac{\lvert\rho_C-\rho_D\rvert g}{12\sigma}}$ (12)
Channel contour radius: $r_\alpha = 0.5 d_{p,I}\left(1-\sqrt{1-\frac{4.7}{La+4.7}}\right)$ (7)	Force due to gravity: $F = \frac{\pi d_{p,0}^3\lvert\rho_C-\rho_D\rvert g}{6}$ (13)
Modified Laplace number: $La = \left(\frac{\lvert\rho_C-\rho_D\rvert g}{\sigma}\right)^{0.6} h_P^{\ 0.2} d_{p,I}$ (8)	Critical film thickness: $\delta_r = 0.267\left(\frac{\pi r^4 \mathrm{H}^2}{6\sigma F}\right)^{\frac{1}{7}}$ (14)

The left column of table 1 shows the *asymmetric film drainage coalescence model*, which depends on the deformation of the drops. Deformation increases with dense packed layer thickness below the drop considered. Two unknown parameters are present in this model: the Hamaker coefficient, H, and the asymmetry parameter, r_V^*. H is set to 10^{-20} N m as proposed by Henschke et al. (2002) for all systems. r_V^* is system specific and can be obtained experimentally.

The right column of table 1 presents the *interfacial mobility film drainage coalescence model.* This coalescence model does not depend on drop size. Instead, the model allows equation (1) to be simplified into equation (11) through the use of equation (9), making h_D independent of $d_{P,I}$.The fitted parameter m is the interface mobility, i.e. the sum of the mobilities due to induced circulation in the adjacent phases and the interfacial tension gradient and is characteristic of each system. When $m = 0$ the velocity at the interfaces on both sides of the draining film is 0, and the surfaces are deemed immobile; when $m = 1.5$ the velocity at one of the interfaces is 0 while the velocity gradient at the other surface is 0. Under these conditions, film drainage, and thus the rate of coalescence, is extremely slow. Other values of m are also possible and correspond to different surface velocities and velocity gradients. Values of m larger than 1.5 correspond to more mobile interfaces.

3. Results and discussion

3.1. Experimental methods

The experimental data used to assess the performance of this model were obtained by Voulgaropoulos (2018) in a two-phase liquid-liquid flow facility discussed in detail in Voulgaropoulos et al. (2016). In the experiments tap water and oil (828 kg m^{-3}, 5.5 mPa s) were used as test fluids. The test section comprised of transparent acrylic pipes with an internal diameter of 37 mm and overall length of around 8 m. Partial dispersions of oil in water were generated at the inlet of the test section using a multi-nozzle mixer. High-speed imaging was employed at three locations along the spanwise dimension of the pipe to enable the identification of the flow patterns. A dual-conductance probe was implemented to measure the local volume fractions and the drop size distributions of the dispersions. Measurements were taken every 2 mm, spanning the whole pipe diameter.

3.2. Results and discussion

Three case studies were investigated (c.f. Table 2). For each case, we solved the mechanistic model twice, implementing a different coalescence model each time, using gPROMS ModelBuilder at intervals of 0.1 m. C_h was taken as 0.01 as suggested by Evripidou et al. (2019) and r_V^* was set to 0.007 as suggested by Pereyra et al. (2013). m was fitted to experimental data obtained at $u_M = 0.52 \text{ m s}^{-1}$ and was found to be 360. The resulting flow profiles were nondimensionalized using the pipe diameter and are presented in Figures 2 and 3.

Table 2: Inlet conditions of the experiments

u_M (m s^{-1})	φ_0
0.52	0.30
	0.45
1.04	0.60

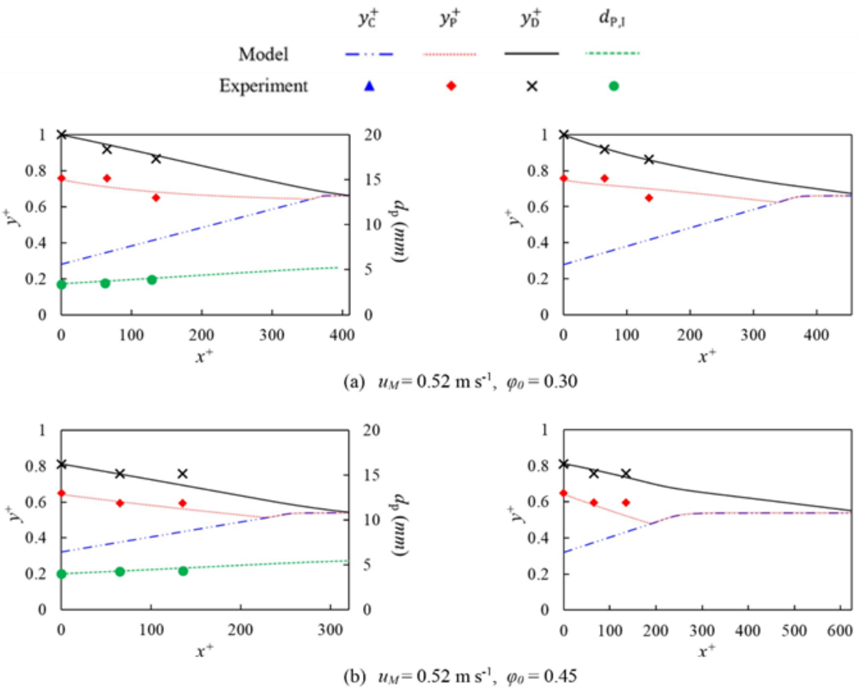

Figure 2: Model predictions of the *asymmetrical film drainage coalescence model* (left) and the *interfacial mobility film drainage coalescence model* (right) for $u_M = 0.52 \text{ m s}^{-1}$.

Figure 2 shows the two case studies at $u_M = 0.52$ m s^{-1} and $\varphi = 0.30$ and 0.45. The two mixtures separate in a similar fashion and both coalescence models predict the separation with reasonable accuracy. The rate of drop-settling is large enough to deplete the SL first. On the contrary, the DPL persists throughout the pipe and coalescence controls the rate of separation.

Although both coalescence models show reasonable agreement with experimental data, the *interfacial mobility film drainage model*, where the coalescence rate is a function of the DPL thickness shows a better fit to the experiments. Despite that, the SL is expected to deplete at similar axial lengths for both cases with deviations of 13% or less in x'^{+} between the predictions of the two models. The predictions of the interfacial mobility film drainage model for the total separation length are consistently larger than the predictions of the asymmetric film drainage model. Specifically, for the case with oil fraction of 0.30, the interfacial mobility film drainage model predicts an x_{sep}^{+} of 455, while the prediction of the asymmetric film drainage model is 9% less at 412. This difference is even larger for the case of oil fraction of 0.45. For this case, the asymmetric film drainage model predicts a separation length of 320, while the other coalescence model predicts $x_{sep}^{+} = 624$, a value that is almost twice as large. The above observations suggest that the models behave in a similar manner at the pipe locations where all four characteristic layers are present, and any major deviations between the two arise past the point of depletion of the SL (i.e. at lengths $x > x'$).

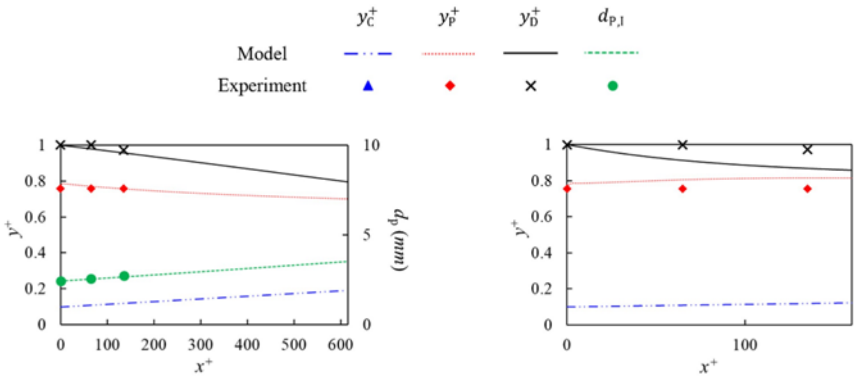

Figure 3: Model predictions of the *asymmetrical film drainage coalescence model* (left) and the *interfacial mobility film drainage coalescence model* (right) for $u_M = 0.52$ m s^{-1} and $\varphi_0 = 0.60$.

Figure 3 presents the results obtained at a mixture velocity of 1.04 m s^{-1} and oil fraction of 0.60. The deviations in the predictions of the two models for this case study are significant. The coalescence model by Henschke et al. (2002) produces reasonable results with deviations of 2% or less to experimental measurements. On the other hand, the *interfacial mobility film drainage model* significantly overestimates the coalescence rate of drops with their homophase. As a result the oil layer acquires a large thickness at the beginning of the pipe. This suggests that the mixture velocity may affect interfacial mobility and that *m* should be fitted for each mixture velocity.

Nevertheless, both models predict depletion of the DPL, which, according to Evripidou et al. (2022), occurs once the thickness of the DPL becomes smaller than the drop diameter along the interface. At this point, settling becomes the limiting separation mechanism and controls the rate of separation. Predictions of the complete flow profile up to the point of total separation are not possible with the current model, as it is only applicable to regions where a DPL is present and coalescence controls the rate of separation.

4. Conclusions

The paper presents a comparison between two coalescence models that can be used in mechanistic models of separating dispersed pipe flows. At the low mixture velocity, both coalescence models capture the drop-interface coalescence adequately. The *interfacial mobility film drainage model* shows better agreement with experimental data, hence may be preferred over the *asymmetric film drainage coalescence model*. The two models result to similar predictions for the length of depletion of the separation layer SL (i.e. $x = x'$), but the *interfacial mobility film drainage model* predicts significantly larger separation lengths x_{sep}. From these observations we concluded that the models behave similarly in pipe locations where all four layers are present, and any major deviations between the two models occur at pipe lengths greater than x' for which we have no experimental data. Therefore, further experimental studies, especially in the region $x > x'$, are needed to provide the necessary information to differentiate between the two coalescence models.

The interfacial mobility coefficient m appears to vary with u_M, but not with oil fraction φ. To the contrary, r_V^* is specific to the oil-water system but independent to both u_M and φ, hence the *asymmetric film drainage model* may be preferred for cases with variable flowrates. Nevertheless, both coalescence models predict the depletion of the DPL at the high mixture velocity, where the present model cannot be used. To account for the depletion of the DPL a different approach must be used such as that described in Evripidou et al. (2022).

Acknowledgements
NE would like to acknowledge Chevron Corporation and UCL for her PhD studentship.

References

Evripidou, N., Voulgaropoulos, V. and Angeli, P., 2019, June. Simplified mechanistic model for the separation of dispersed oil-water horizontal pipe flows. In BHR 19th International Conference on Multiphase Production Technology. OnePetro.

Evripidou, N., Avila, C. and Angeli, P., 2022. A mechanistic model for the prediction of flow pattern transitions during separation of liquid-liquid pipe flows. International Journal of Multiphase Flow, p.104172.

Henschke, M., Schlieper, L.H., Pfennig, A., 2002. Determination of a coalescence parameter from batch-settling experiments. Chem Eng J 85, 369-378.

Jeelani, S. A. K., Hartland, S. 1994 Effect of interfacial mobility on thin film drainage. J. Colloid Interface Sci., 164, 296-308.

Pereyra, E., Mohan, R.S., Shoham, O., 2013. A simplified mechanistic model for an oil/water horizontal pipe separator. Oil and Gas Facilities, 2 (03): 40-46.

Voulgaropoulos, V., Zhai, L.-S., Ioannou, K., Angeli, P., 2016. Evolution of unstable liquid-liquid dispersions in horizontal pipes. 10th North American Conference on Multiphase Technology. BHR Group. Banff, 8-10 June.

Voulgaropoulos, V., 2018. Dynamics of spatially evolving dispersed flows. PhD dissertation, University College London, London, UK.